第百七十一號

（昭和十三年十一月發行）

抄　錄

鐵・ニツケル・アルミニウム系に於ける新變態 $\alpha \rightarrow \alpha+\alpha'$ に就て

囑託　理學士　木　内　修　一

鐵・ニツケル・アルミニウム系の合金は强力なる耐久磁性を有する點に於て世の注目をひき最近多くの研究結果の報告が續出してゐる．その三元系狀態圖には W. Köster の研究（1933年）があり同氏は氏の狀態圖からの考察によりこの强力なる抗磁力は α-相（體心立方格子）から γ-相（面心立方格子）が析出するためであると結論してゐるが，これは著者の研究結果と一致しない．即ち，その試料の燒鈍組織は不均一組織を示して均一固溶體より他の相が析出した事を示してゐるがそれをX線によつて分析して見ると單に體心立方晶に屬してゐる格子の干涉線が見られるのみであつて何等 γ-相の干涉線が現れて來ない．然るに一方顯微鏡下に於ては２つの相が見られ且つその各々の結晶粒の形狀，大さ及び分量より考へて必らず兩者のX線干涉線が觀られなくてはならない．依つて著者はこの析出相は γ-相と異なる別個の相であるものと考へ燒鈍試料の示すX線干涉線より判斷して該析出相は α-相に類似した相であるとの想像のもとに假りに α'-相と名づけこの系の示す强力なる抗磁力は α-相より α'-相を析出するためならんと考へた．（1934年．4月．日本數學物理學會年會記事參照）．そして其後，鐵・ニツケル・アルミニウム三元系を研究した結果この α'-相は金屬間化合物 NiAl の固溶體と同一物であるといふ結論に達したのである．（1935年．10月．數．物．例會記事參照）尙その研究の結果從來 $(\alpha+\gamma)$ 不均一系と見做された部分が $(\alpha+\alpha')$, $(\alpha'+\gamma)$, $(\alpha+\gamma)$ 及び $(\alpha+\alpha'+\gamma)$ の諸部分に分けられ强力なる抗磁力は室溫に於て $(\alpha+\alpha')$ 及び $(\alpha+\alpha'+\gamma)$ となる組成のものに於て見られる事がわかつた．更に抗磁力の極大値は $(\alpha+\alpha')$ となる組成のものに於て見られるのでこの三元系に於て見られる强力なる抗磁力は主として $\alpha \rightarrow (\alpha+\alpha')$ の變化に基く事がわかつた．（航空研究所彙報 152 卷 179 頁參照．）*

*尙同じ年の暮に發行された Nature 誌上に於て A. J. Bradley 及び A. Taylor が著者の得たものと同樣な狀態圖を提出し續いてその論文に於て著者の研究結果が一致してゐる事を述べてゐる．（Proc. Roy. Soc. London. 166卷 (1938) 360頁 參照．）

さてKösterの狀態圖と著者の狀態圖との相違點は要するにKösterはα-鐵とNiAlが完全に固溶體を作るものであると假定してこの系は單にα-相及びγ-相とより成るものと考へた事に基く．又この三元系が多くの學者によりX線で研究されたにも拘らずそのX線分析が困難なるためにKöster狀態圖の誤りを發見出來なかつたのである．即ち，α-相とα′-相は共に體心立方格子であつてその格子常數が接近してゐるので(α+α′)不均一相とα-相との識別が困難である．普通の燒鈍組織に於ては(α+α′)不均一相は單に幅の廣くなつたα-相と同樣なX線干涉線を示す．從來のX線研究者は皆これはα-相からγ-相が析出するため結晶格子が歪を受けたためであると說明してゐた，若し然らばこの試料を完全に燒鈍すれば干涉線の幅が減少してγ-相の干涉線が出て來なければならないが事實は然らず，更にこの說明は顯微鏡組織との比較考察に於て種々矛盾を生じて來るのである．燒鈍によりX線干涉線の幅の廣くなる現象は著者の提出した狀態圖により說明つくのである．即ち，α→α+α′の變化のためNi及びAlの濃度が異り從つて格子常數が異る種々の體心立方格子が出來るために幅の廣い體心立方格子の干涉線が現れて來る．(勿論α-相からα′-相が析出するため結晶格子が歪を受けて干涉線の幅を增すがその影響は前者のそれに比べて小さい) 果して然らば燒鈍過程を完全に進行せしめればX線干涉線は各々2本の線に分離し(α+α′)の平衡を示すものと考へられるがこれは著者の研究に依つて確められたのである．

No. 171.

(Published November, 1938.)

A New Transformation in the Iron-Nickel-Aluminium System.

By

Syûiti KIUTI, *Rigakusi*,

Research Associate of the Institute.

§ 1. Introduction.

An alloy of iron, nickel and aluminium which contains about 8～14 per cent aluminium and 25～40 per cent nickel has become a very important one, as it has large coercive force. After its discovery, the structure and the cause of high coercivity of this alloy have been studied by many workers. Among them W. Köster, in his metallographical investigation of the ternary system iron-nickel-aluminium[1], concluded that the large coercive force of this alloy is due to the precipitation of γ-phase (a face-centered cubic lattice) from the matrix of α-phase (a body-centered cubic lattice)[2]. Afterwards R. Glocker, H. Pfister and P. Wiest[3] made an X-ray study of this alloy confirming the results of W. Köster. They also concluded that the structure which shows the large coercive force is in an intermediate state prior to the precipitation of γ-phase from the matrix of α-phase. On the other hand, W. G. Burgers and J. L. Snoek[4] made an X-ray investigation of a single crystal of this alloy and concluded that in the state of the highest coercive force, the segregation of the undercooled metastable homogeneous α-phase into a stable α- and

(1) W. Köster, Archiv. Eisenhüttenwes., 7 (1933), 257.
(2) W. Köster, Stahl u. Eisen, 53 (1933), 849.
(3) R. Glocker, H. Pfister and P. Wiest, Archiv. Eisenhüttenwes., 8 (1935), 561.
(4) W. G. Burgers and J. L. Snoek, Physica, 2 (1935), 1064.

γ-phase of different composition is just in the preliminary stage, resulting in the formation of a highly stressed state in the lattice.

At any rate, the conclusions of these authors rest on the diagram proposed by W. Köster. But according to the result of the present author's work[5] by X-ray and microscopic analyses of the iron-nickel-aluminium magnet alloys, their results did not agree with the new data. That is to say, the author observed the precipitation of γ-phase in some specimens, but those which have maximum values of coercive force did not show any precipitation of this phase, even when in the thoroughly annealed state. Hence it is highly probable that the high coercive force of this alloy is due to some other nature. In order to clarify this problem the author made X-ray and microscopic investigations of the ternary system iron-nickel-aluminium and a new phase was introduced in the diagram[6].

In this paper the newly found phase in the diagram is discussed, and a particular account of the ternary diagram will be given later.

§ 2. Introduction of a new phase (α') in the iron-rich alloys of the iron-nickel-aluminium system.

Specimens which are shown in Fig. 1 *a*, Fig. 1 *c*, Fig. 2 *a* are obviously of heterogeneous structure. Formerly it was supposed that this heterogeneous structure was due to the precipitation of γ-phase from the α-solid solution[1]. But according to the author's X-ray analysis no γ-phase appeared, in spite of the fact that the X-ray interference lines of this precipitated phase must appear. Thus the precipitated phase has to be a new phase[5], and the author named it α'-phase, for which by subsequent investigation it has been proved to be a solid solution of the intermetallic compound NiAl[6]. Thus in the iron-nickel-aluminium

(5) S. Kiuti, Read at the annual meeting of the Physico-Mathematical Society of Japan. (April 1934).

(6) S. Kiuti, Read at the monthly meeting of the Physico-Mathematical Society of Japan (19 Oct. 1935), also at the autumn meeting of the Society of the Aeronautical Science of Nippon which was held in Sendai (31 Oct. 1936), Cf. also Journ. Aero. Res. Inst. Tôkyo, Imp. Univ. 152 (1937), 179.

Fig. 1 a
Fe 59
Ni 30
Al 11
1300°→w.q.
1200°→s.c.
×240

Fig. 1 e
Fe 51
Ni 40
Al 9
1250°→w.q.
×240

Fig. 1 b
Fe 59
Ni 30
Al 11
1300°→w.q.
1200°→w.q.
×240

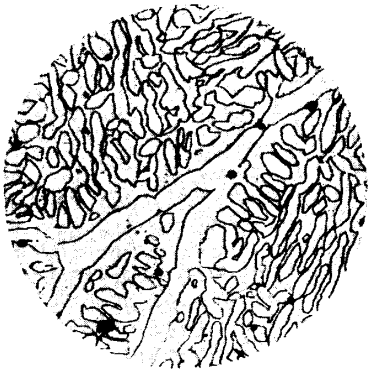

Fig. 1 f
Fe 51
Ni 40
Al 9
1300°→w q.
×240

Fig. 1 c
Fe 55.5
Ni 32.5
Al 12
1300°→w.q.
1100°→s.c.
×240

Fig. 1 g
Fe 70
NiAl 30
1000°×
10h→s.c.
×240

Fig. 1 d
Fe 55.5
Ni 32.5
Al 12
1300°→w.q.
1100°→w.q.
×240

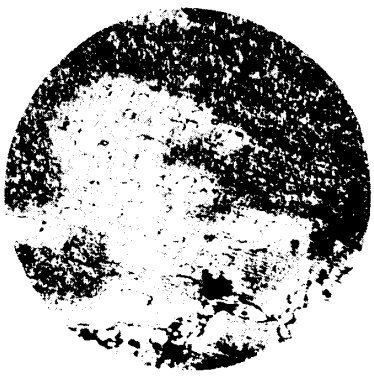

Fig. 1 h
Fe 60
NiAl 40
1000°×
10h→s.c.
×240

Fig. 2 a
Fe 53
Ni 35
Al 12
1000°×10h
→s.c.
×240

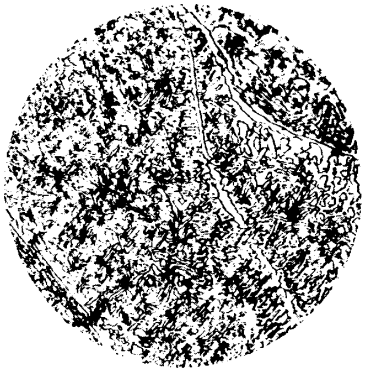

Fig. 2 e
Fe 50
Ni 40
Al 10
1000°×1h
→s.c.
×240

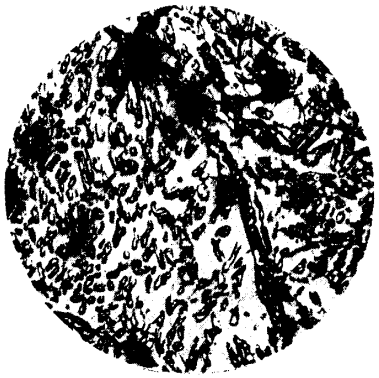

Fig. 2 b
Fe 54
Ni 35
Al 11
1000°×10h
→s.c.
×240

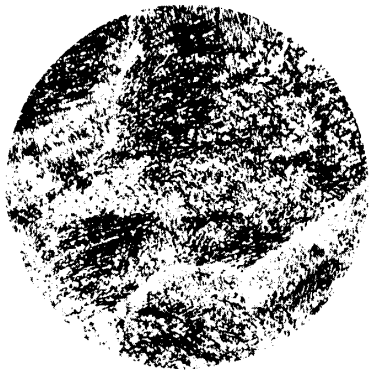

Fig. 2 f
Fe 51
Ni 40
Al 9
1000°×1h
→s.c.
×240

Fig. 2 c
Fe 55
Ni 35
Al 10
1000°×10h
→s.c.
×240

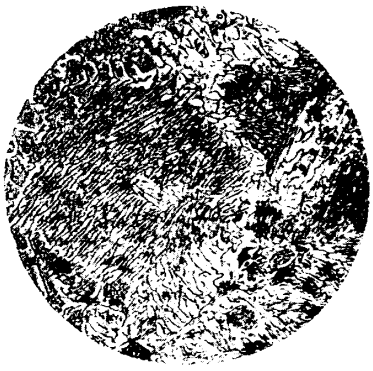

Fig. 2 g
Fe 60
Ni 32
Al 8
1000°×1h
→s.c.
×240

Fig. 2 d
Fe 56
Ni 35
Al 9
1000°×1h
→s.c.
×240

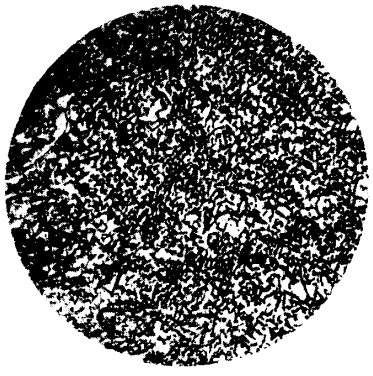

Fig. 2 h
Fe 45.5
Ni 42
Al 12.5
1000°×1h
→s.c.
×240

magnet alloys the following three phases exist, α-phase of α-iron, γ-phase of nickel and α'-phase of NiAl. At high temperatures the α'-phase of NiAl and the α-phase of iron completely dissolve each other in any percentage, but when the temperature is lowered a heterogeneous field $(\alpha+\alpha')$ appears the α'-phase of NiAl becomes an independent one from the α-phase of iron. The point where the author's diagram differs from that of W. Köster is that the latter assumed this ternary system to be composed of only the two phases, α-phase of iron and γ-phase of nickel. Further the X-ray analysis of R. Glocker, H. Pfister and P. Wiest confirmed the result of W. Köster assuming that there exist only α- and γ-phase. But the heterogeneous field which W. Köster supposed to be composed of α- and γ-phase is now to be divided into those parts of $(\alpha+\alpha')$-, $(\alpha'+\gamma)$-, $(\alpha+\gamma)$- and $(\alpha+\alpha'+\gamma)$-phase. (In the study of a former investigator[7] there exists a superlattice Fe_2NiAl, but such a structure has not been observed in the present work. Further, as no new X-ray interference lines were observed, a ternary intermetallic compound in the iron-rich iron-nickel-aluminium system was supposed to be absent.)

§ 3. Mutual solubility of the α-iron and the intermetallic compound NiAl.

NiAl, which is an intermetallic compound of nickel and aluminium, has a crystal structure of CsCl type and its lattice constant is about 2·88 Å. Thus it has a body-centered cubic lattice with a superstructure of a simple cube, and the α-iron has also a body-centered cubic lattice, the lattice constant being about 2·86 Å. Hence the α-iron (α-phase) and NiAl (α'-phase) are very similar in structure and very likely to form the whole range of a homogeneous solid solution, but in reality this is not the case.

When iron is added to NiAl, it dissolves completely in the α'-phase of NiAl up to 45 per cent, but when its content is further increased, the coexistence of two phases is observed. When NiAl is added to

(7) Zeits. tech. Phys., **17** (1936), 33.

iron, it completely dissolves up to 10 per cent, but when its percentage is further increased, the coexistence of two phases is also observed. The α-phase of α-iron and the α'-phase of NiAl dissolve each other at higher temperatures at all percentages, but when the temperature is lowered, there appear solubility limits, forming a heterogeneous field as is shown in Fig. 11.

Since α'-phase is a body-centered cubic lattice with the atoms in ordered arrangement, it can not be anything else but a kind of α-phase having a superstructure. Consequently at higher temperatures, when the ordered arrangement of atoms has a tendency to become disordered by heat agitation, the difference of the α- and α'-phases decreases and these two phases dissolve each other. But when the temperature is lowered the difference of the α- and α'-phases can not be negligible and α'-phase becomes independent of the α-phase.

§ 4. Occurrence of a heterogeneous concentration by the $\alpha \rightarrow \alpha + \alpha'$ Change.

The α'-phase of NiAl and the α-phase of α-iron are both body-centered cubic lattices and are soluble at higher temperatures at al percentages, but at low temperatures they have limits of solubility, forming as already described a heterogeneous structure due to the mixture of two phases.

Now the process of precipitation phenomenon is considered. At first the movement of atoms in the solid state occurs and solute atoms show a local concentration. Next, the change of the crystal structure occurs at parts where solute atoms are assembled, and new X-ray interference lines due to this newly constituted crystal lattice are observed. Thus the precipitation phenomenon in the ordinary sense means (1) the local concentration of the solute atoms, and (2) the change in the crystal lattice where the solute atoms are assembled. But when the crystal lattice of the solute atoms are of the same type as that of the solvent atoms, the second change does not occur. In this case the change in the

lattice constant is observed as the result of the change in concentration. The precipitation of new phase due to the $\alpha \rightarrow \alpha + \alpha'$ change belongs to the latter case. The local concentration of nickel- and aluminium-atoms results a change in lattice constant. But under ordinary heat treatment, the $\alpha \rightarrow \alpha + \alpha'$ change does not go to completion, and as the precipitation phenomenon does not occur uniformly, the lamp annealed specimen shows a heterogeneous structure which is observed by X-ray analysis. Thus the X-ray photograph of the lamp annealed specimen shows the diffused interference lines[8] as is shown in Fig. 5 *h*, Fig. 5 *i*. (In the powder annealed specimens, in which the precipitation phenomenon is supposed to be uniformly completed[9], the X-ray interference lines are split in two indicating the coexistence of the two body-centered cubic lattices as shown in Fig. 7 *a*, Fig. 7 *b*, Fig. 7 *d*, Fig. 7 *e*.)

§ 5. On the method of X-ray analysis.

In the present X-ray analysis specimens which were heat treated in the lump-form were mostly used, and as the filing operation generally introduces cold-working and change in the structure[10], the specimens were examined in the lump-form by the Seemann-Bohlin method and the back reflection method, and rotated about the axis perpendicular to the finished surface. In order to avoid the effect of completion, the finished surface was etched off about 0·2 mm. with dilute nitric acid. The dissolution of the surface does not take place uniformly, the α-phase being more rapidly dissolved than the α'-phase. But this heterogeneous

(8) The width of the X-ray interference lines is partly due to the stress which is caused by the precipitation of the new phase, and mostly to the heterogeneous concentration as will be explained later.

(9) In the powdered specimens the resistance against the diffusion of atoms is very much reduced, and further there are some advantageous circumstances for the precipitation phenomenon. (Cf. G. Tammann: Der Einfluss der Kaltbearbeitung auf die Temperature des Beginns der Grauglut. Ann. d. Phys., **15** (1932), 317).

(10) The particular account of this circumstance was read at the monthly meeting of the Physico-Mathematical Society of Japan (Nov. 1934); Cf. also S. Kiuti, Journ. Soc. Aero. Sci. Nippon, **4** (1937), 39.

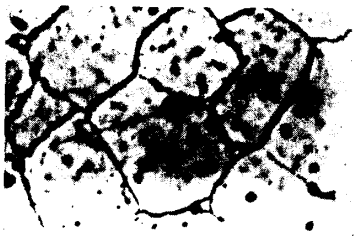

Fig. 3 a
Fe 30
NiAl 70
annealed
×60

Fig. 3 f
Fe 80
NiAl 20
annealed
×60

Fig. 3 b
Fe 40
NiAl 60
annealed
×60

Fig. 3 g
Fe 90
NiAl 10
annealed
×60

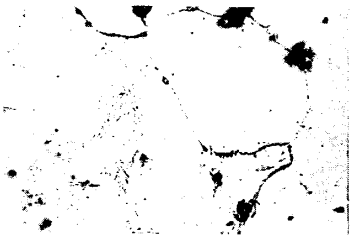

Fig. 3 c
Fe 50
NiAl 50
annealed
×60

Fig. 3 h
Fe 95
NiAl 5
annealed
×60

Fig. 3 d
Fe 60
NiAl 40
annealed
×60

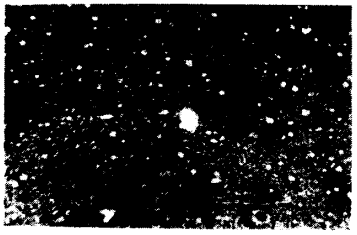

Fig. 3 i
Fe 70
Ni 20
Al 10
annealed
×360

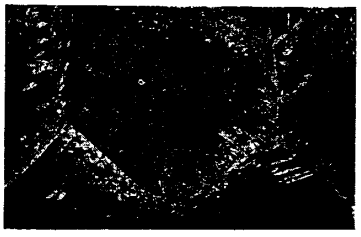

Fig. 3 e
Fe 70
NiAl 30
annealed
×60

Fig. 3 j
Fe 60
Ni 30
Al 10
annealed
×360

Fig. 4 a
Fe 40
Ni 44
Al 16
annealed
×60

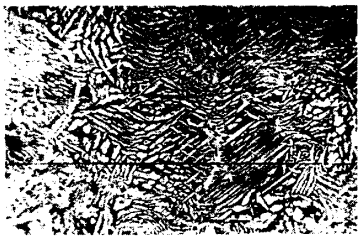

Fig. 4 f
Ni 81
Al 19
annealed
×60

Fig. 4 b
Fe 40
Ni 45
Al 15
annealed
×60

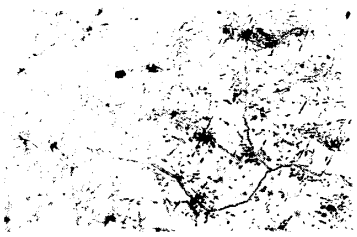

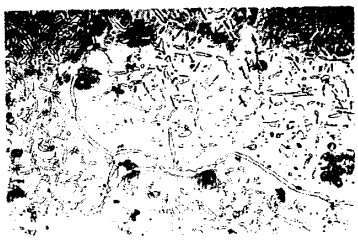

Fig. 4 g
Fe 10
Ni 73
Al 17
annealed
×60

Fig. 4 c
Fe 40
Ni 46
Al 14
annealed
×60

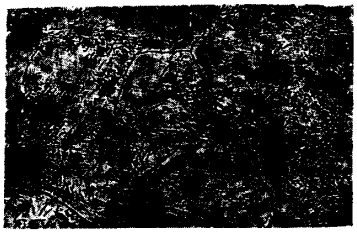

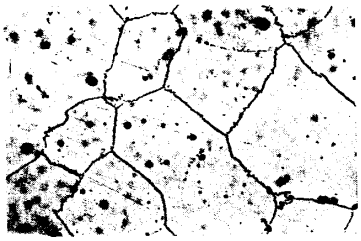

Fig. 4 h
Fe 30
Ni 55
Al 15
annealed
×60

Fig. 4 d
Fe 40
Ni 47
Al 13
annealed
×60

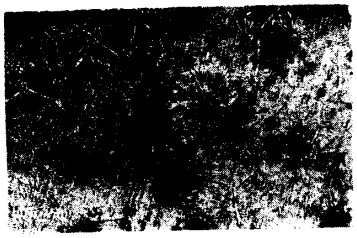

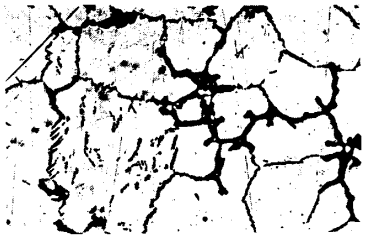

Fig. 4 i
Fe 30
Ni 56
Al 14
annealed
×60

Fig. 4 e
Fe 40
Ni 48
Al 12
annealed
×60

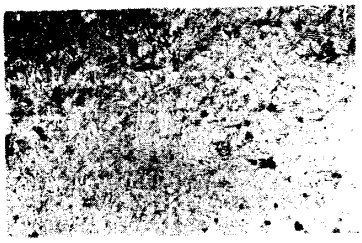

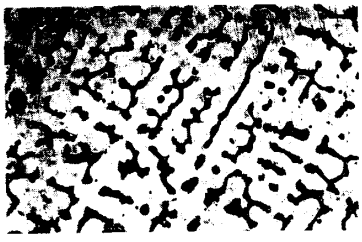

Fig. 4 j
Fe 30
Ni 57
Al 13
annealed
×60

Fig. 5a Fe 95 NiAl 5 1300°→w.q. etch. rot. (Co-ray)

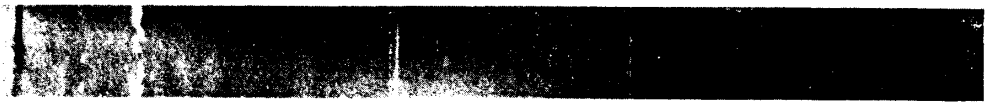

Fig. 5b Fe 80 NiAl 20 1300°→w.q. etch. rot. (Co-ray)

Fig. 5c Fe 70 NiAl 30 1300°→w.q. etch. rot. (Co-ray)

Fig. 5d Fe 60 NiAl 40 1300°→w.q. etch. rot. (Co-ray)

Fig. 5e Fe 50 NiAl 50 1300°→w.q. etch. rot. (Co-ray)

Fig. 5f Fe 40 NiAl 60 1300°→w.q. etch. rot. (Co-ray)

Fig. 5g Fe 95 NiAl 5 1000°×10^{h}→s.c. etch. rot. (Cr-ray)

Fig. 5h Fe 70 NiAl 30 1000°×10^{h}→s.c. etch. rot. (Cr-ray)

Fig. 5i Fe 60 NiAl 40 1000°×10^{h}→s.c. etch. rot. (Cr-ray)

Fig. 5j Fe 40 NiAl 60 1000°×10^{h}→s.c. etch. rot. (Cr-ray)

Fig. 6a Fe 54 Ni 35 Al 11 1300°×1h→w.q. 1200°×1h→s.c. etch. rot. (Co-ray)

Fig. 6b Fe 54 Ni 35 Al 11 1300°×1h→w.q. 1200°×1h→w.q. etch. rot. (Co-ray)

Fig. 6c Fe 51 Ni 40 Al 9 1000°×10h→s.c. etch. rot. (Co-ray)

Fig. 6d Fe 51 Ni 40 Al 9 1250°×1h→w.q. etch. fix. (Co-ray)

Fig. 6e Fe 51 Ni 40 Al 9 1250°×1h→w.q. 1300°×30′→w.q. etch. fix. (Co-ray)

Fig. 6f Fe 55 Ni 35 Al 10 1300°×1h→w.q. 1100°×1h→w.q. etch. rot. (Co-ray)

Fig. 6g Fe 55 Ni 35 Al 10 1300°×1h→w.q. 1100°×1h→s.c. etch. rot. (Co-ray)

Fig. 6h Fe 53 Ni 35 Al 12 1300°×1h→w.q. 1100°×1h→w.q. fix. (Co-ray)

Fig. 6i Fe 53 Ni 35 Al 12 1300°×1h→w.q. 1100°×1h→w.q. rot. (Co-ray)

Fig. 6j Fe 53 Ni 35 Al 12 1300°×1h→w.q. 1100°×1h→s.c. rot. (Co-ray)

Fig. 7a Fe 70 NiAl 30 powder annealed (Debye-Scherrer camera)

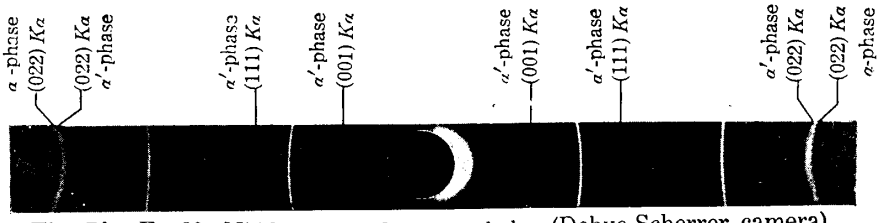

Fig. 7b Fe 60 NiAl 40 powder annealed (Debye-Scherrer camera)

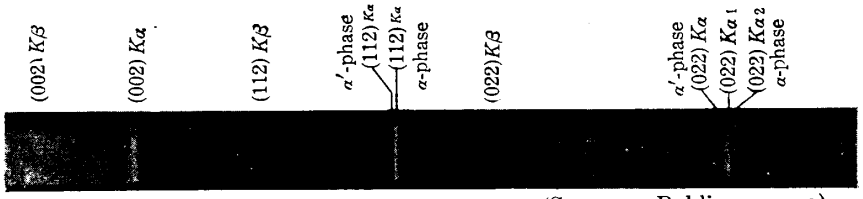

Fig. 7c Fe 80 NiAl 20 powder annealed (Seemann-Bohlin camera)

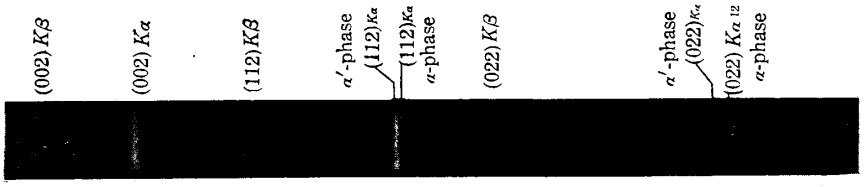

Fig. 7d Fe 70 NiAl 30 powder annealed (Seemann-Bohlin camera)

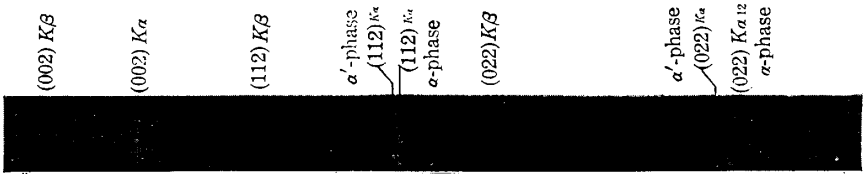

Fig. 7e Fe 60 NiAl 40 powder annealed (Seemann-Bohlin camera)

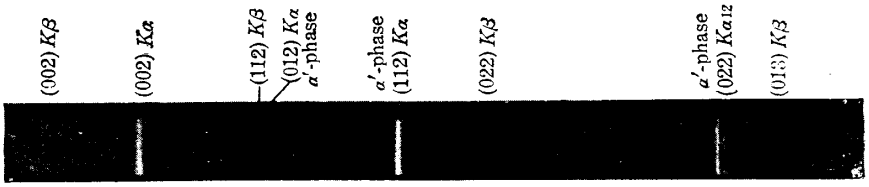

Fig. 7f Fe 50 NiAl 50 powder annealed (Seemann-Bohlin camera)

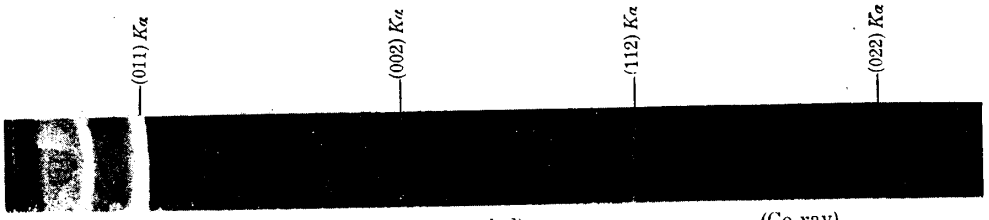

Fig. 8a Fe 61 Ni 30 Al 9 (lump-annealed) (Co-ray)

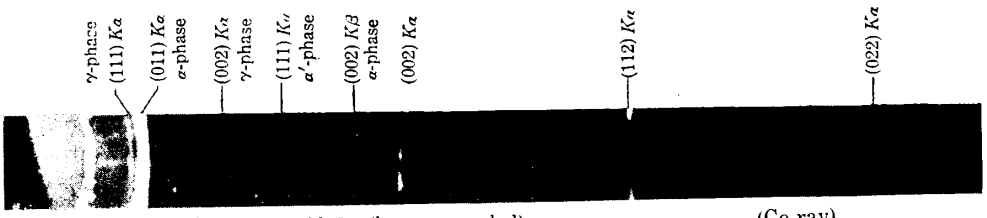

Fig. 8b Fe 62 Ni 30 Al 8 (lump-annealed) (Co-ray)

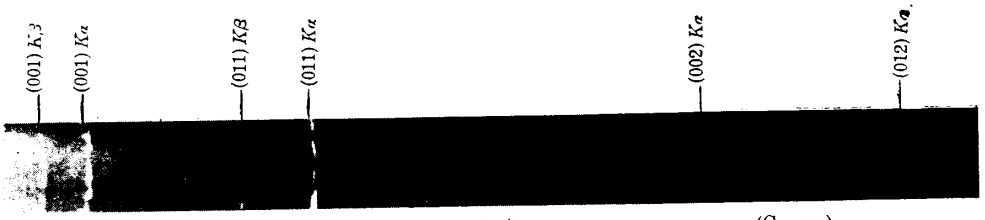

Fig. 8c Fe 61 Ni 30 Al 9 (lump-annealed) (Cr-ray)

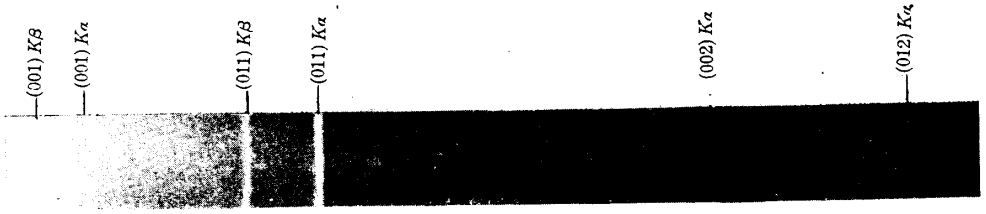

Fig. 8d Fe 60 Ni 30 Al 10 (lump-annealed) (Cr-ray)

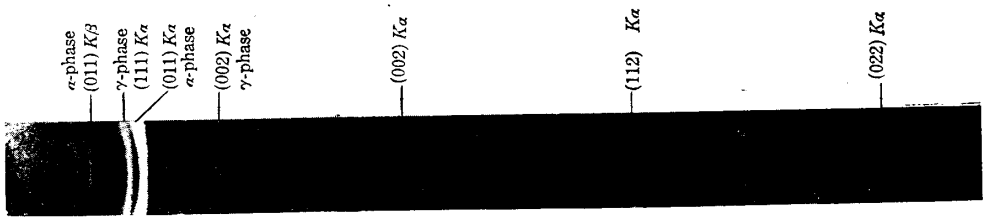

Fig. 8e Fe 62 Ni 30 Al 8 (stress-annealed) (Co-ray)

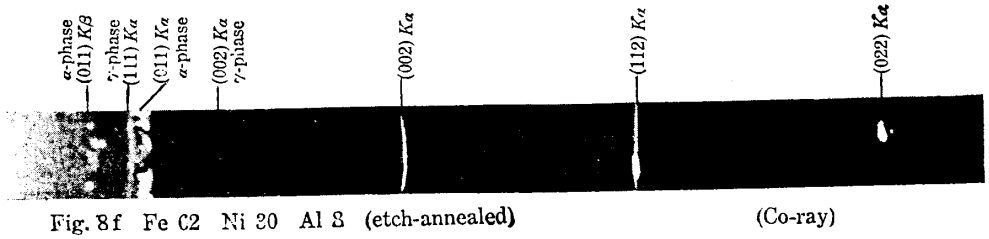

Fig. 8f Fe 62 Ni 30 Al 8 (etch-annealed) (Co-ray)

degree of etching remained within a thin layer, the effect of which is observed in the X-ray interference lines of small glancing angles. In large glancing angles, the X-rays, penetrated the thin layer above mentioned, have taken part in the interference phenomenon, and the effect of heterogeneity in etching did not appear any more. On this account the interference lines were examined at larger glancing angles. But as the superlattice lines were more intense in smaller glancing angles, the interference lines of small glancing angles were also examined in the investigation of the superstructure, taking care of the above related circumstances. The method of X-ray powder analysis was also used in the differentiation of α- and α'-phases. As will be described later, the lump-annealed specimens which belong to the $(\alpha+\alpha')$- and $(\alpha+\alpha'+\gamma)$-fields in Fig. 12, all show diffused interference lines of the body-centered cubic lattice, instead of the interference lines of the two body-centered cubic lattices. By annealing the powdered specimens in vacuum, the author succeeded in observing the interference lines which belong to the two body-centered cubic lattices.

§ 6. Sectional diagram of the Fe-NiAl system.

In order to study the sectional diagram of the system Fe-NiAl, alloys prepared by adding iron to the intermetallic compound NiAl were investigated. At first microscopic structure of the annealed specimens were studied and the heterogeneous field at room temperature was determined. Specimens which contain 10 per cent, 20 per cent, 40 per cent and 45 per cent of iron showed homogeneous structure under the microscope. In X-ray analysis they all showed sharp interference lines which belong to the α'-phase of NiAl. The α'-phase shows the interference lines which belong to a body-centered cubic lattice and in addition the superlattice lines of (001), (111) etc., the intensity of these lines decreasing with the content of iron. But when the content of iron is further increased, heterogeneous structure appears, the photomicrographs of which are shown in Figs. 3 *a*—*h*, Fig. 1 *g*, Fig. 1 *h*. The

X-ray photographs of these specimens, which are shown in Fig. 5*h*, Fig. 5*i*, show diffused interference lines. This indicates the occurrence of heterogeneous concentration, and when the specimens are powder-annealed, the diffused interference lines above mentioned are split in two, showing the coexistence of two body-centered cubic lattices with a slightly different lattice constant. (It was formerly supposed that the diffused interference lines are due to the stress prior to the precipitation of the γ-phase. But as the powder-annealed specimens show two body-centered cubic lattices instead of the precipitation of γ-phase, this opinion does not hold). The heterogeneous concentration above stated is due to the $\alpha \rightarrow \alpha+\alpha'$ change. The lattice constant of iron is 2·86 Å while that of NiAl is 2·88 Å, and the occurrence of the heterogeneous concentration due to the $\alpha \rightarrow \alpha+\alpha'$ change causes the heterogeneity in the lattice constant, which is observed by the diffused interference lines.

This heterogeneous field extends to 87·5 per cent of iron. A specimen which contains 90 per cent of iron shows the homogeneous α-solid solution. (The martensitic structure which is seen in the microphotograph is supposed to be due to the occurrence of the A_3-transformation at a low temperature). The superlattice lines are entirely absent in this α-solid solution as shown in Fig. 5*a*, Fig. 5*g*. (C_r K_α radiation was used to bring out the most dominant superlattice line of (001)).

The same specimens were next examined by quenching. As is shown in Fig. 11, the range of the heterogeneous field of $(\alpha+\alpha')$ is narrowed at high temperature, the fact of which was confirmed by the examination of the quenched specimens. When the temperature is above 1300° all of the specimens showed homogeneous structure under the microscope, and the X-ray investigation also showed the homogeneous phase Fig. 5*a*—Fig. 5*f*. Thus it is seen that the heterogeneous phase of $(\alpha+\alpha')$ does not exist above 1300°; in these temperatures the α-phase of iron and the α'-phase of NiAl make a solid solution in all proportion.

Next the results of the dilatometric and magnetic analyses are described. When NiAl is added to iron, the A_3-transformation shows

a remarkable irreversibility, the Ac_3 appears far above Ar_3. These transformation points at first drop and then rise and connect with the A_4-transformation point, making a loop analogous to the case of iron chromium alloys. By the further addition of NiAl to iron, the transformation point of iron vanishes, and as grain refinement does not occur, large grains appear under microscope as shown in Fig. 3*f*, Fig. 3*c*. The sectional diagram of the Fe-NiAl system is shown in Fig. 11.

§ 7. The diagram of the Ni-NiAl system.

The diagram of the Ni-Al system was first studied by C. G. Gwyer[11], and recently an X-ray investigation of this alloy system has been published by A. J. Bradley and A. Taylor[12], whose diagram agrees with that established by the author. The solid solution of aluminium in nickel shown by Gywer has a miscibility gap at a lower temperature. The phase, which is a face-centered cubic solid solution of aluminium in nickel extends to 94 per cent of nickel at room temperature. But when the content of aluminium is increased a heterogeneous portion of $\gamma+\gamma'$ appears. The γ'-phase, which is a face-centered cubic solid solution closely corresponding to the chemical formula Ni_3Al has a superstructure of a simple cube, nickel atoms occupying centers of cube-faces and aluminium atoms cube-corners. The heterogeneous field of $\gamma+\gamma'$ exists only below 1100°, above which the structure as quenching is homogeneous. The range of the heterogeneous field extends to 87 per cent nickel. The α'-phase of NiAl has a crystal structure of CsCl-type, and a eutectic reaction occurs at about 1370° with this phase and the γ-phase of Ni. The γ-phase dissolves a large quantity of aluminium to form a solid solution, and the α'-phase of NiAl also dissolves nickel in solid solution, the solubility curves being shown in Fig. 11. As an example, a specimen of 14 per cent alumimium was taken, which showed a heterogeneous structure when quenched from 1300°, but a homogeneous structure when

(11) C. G. Gwyer, Z. anorg. allg. Chem. **57** (1908) 133.
(12) A. J. Bradley, A. Taylor, Proc. Roy. Soc. London, A, **159** (1937) 56.

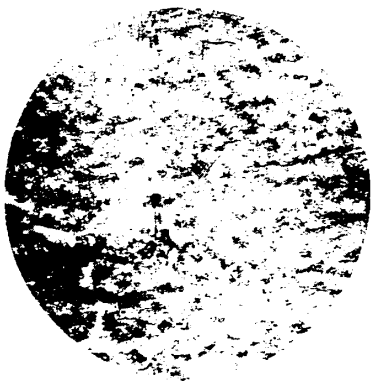

Fig. 9 a
Fe 85
Ni 10
Al 5
annealed
×240

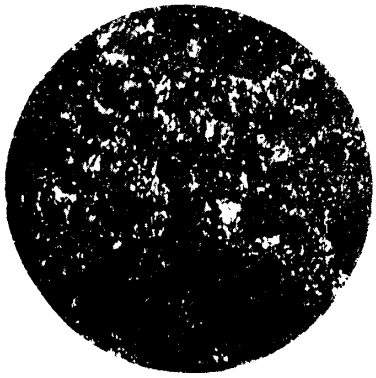

Fig. 9 e
Fe 75
Ni 20
Al 5
annealed
×240

Fig. 9 b
Fe 82.5
Ni 12.5
Al 5
annealed
×240

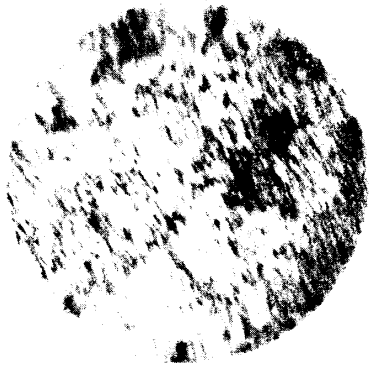

Fig. 9 f
Fe 74
Ni 21
Al 5
annealed
×240

Fig. 9 c
Fe 80
Ni 15
Al 5
annealed
×240

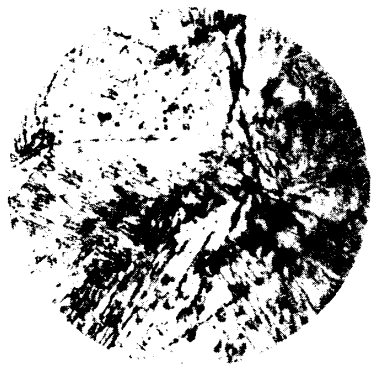

Fig. 9 g
Fe 70
Ni 25
Al 5
annealed
×240

Fig. 9 d
Fe 77.5
Ni 17.5
Al 5
annealed
×240

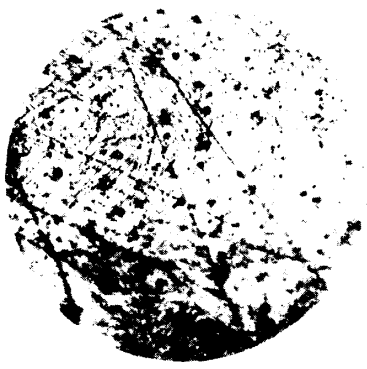

Fig. 9 h
Fe 64
Ni 31
Al 5
annealed
×240

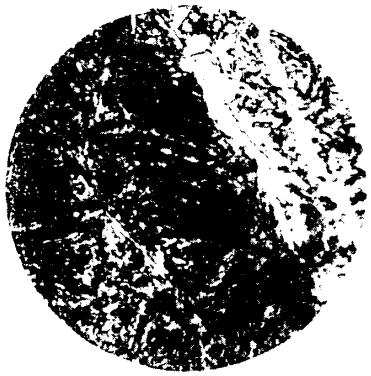

Fig. 10 a
Fe 60
Ni 30
Al 10
annealed
×240

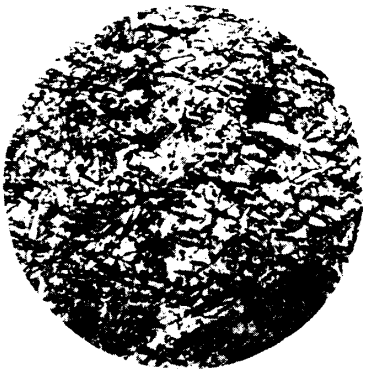

Fig. 10 e
Fe 47.5
Ni 40
Al 12.5
annealed
×240

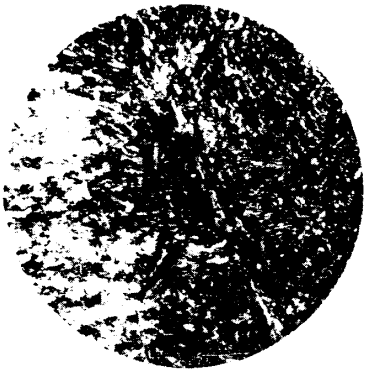

Fig. 10 b
Fe 59
Ni 31
Al 10
annealed
×240

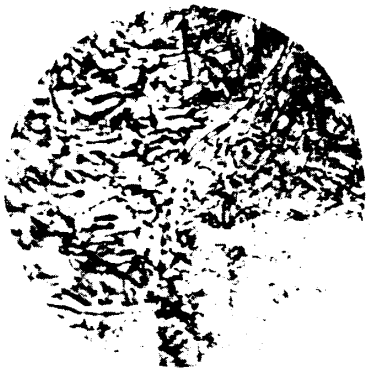

Fig. 10 f
Fe 46.5
Ni 41
Al 12.5
annealed
×240

Fig. 10 c
Fe 58
Ni 32
Al 10
annealed
×240

Fig. 10 g
Fe 44.5
Ni 43
Al 12.5
annealed
×240

Fig. 10 d
Fe 57
Ni 33
Al 10
annealed
×240

Fig. 10 h
Fe 43.5
Ni 44
Al 12.5
annealed
×240

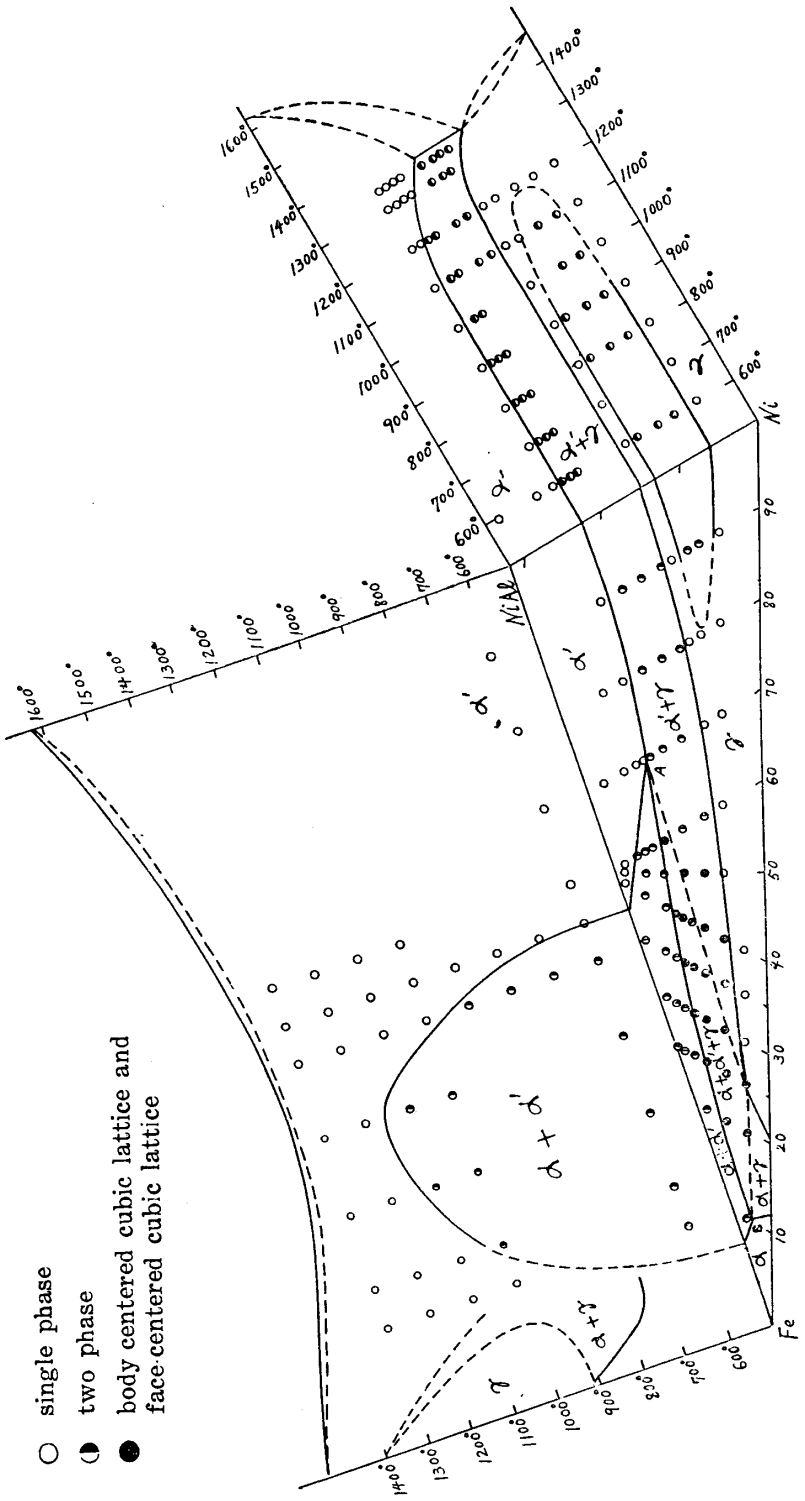

Fig. 11 (600°C)

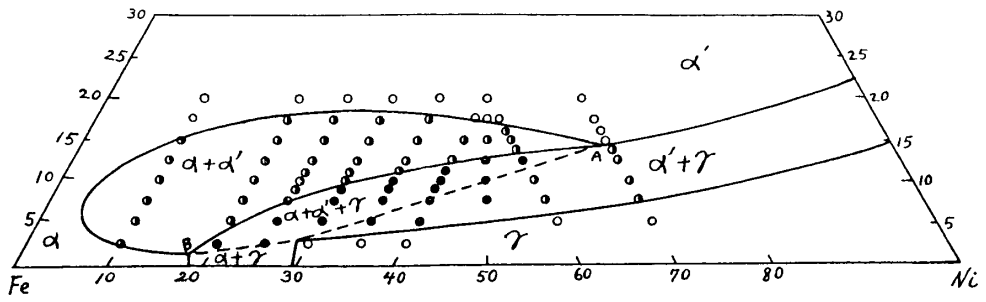

Fig. 12 (R. T.)

annealed. The latter (homogeneous structure) is the γ-phase of nickel, and the former (heterogeneous structure), which lies between 13 per cent to 17 per cent aluminium at 1350° and 15 per cent to 22 per cent aluminium at room temperature, is a mixture of α'- and γ-phase.

§ 8. The phase boundary of the Fe-Ni-Al system.

The phase boundary of the ternary system at room temperature is shown in Fig. 12. With thoroughly annealed specimens, the homogeneous and heterogeneous fields[13] were determined by the microscope. It is seen that the curve, which marks the phase boundaries of the heterogeneous portion, shows an abrupt change of curve. (Point A, B in Fig. 12) This indicates that this heterogeneous field is not simple in nature. The same specimens were then examined by X-ray and the heterogeneous field above obtained was divided into those parts of $(\alpha+\gamma)$-, $(\alpha+\alpha')$-, $(\alpha'+\gamma)$- and $(\alpha+\alpha'+\gamma)$-phase[14]. Some X-ray patterns as well as the photomicrographs are shown in Figs. 1—10. The particular account of the X-ray analysis will be later given. Points A, B, showing an abrupt change of curve are now to be the corners of the region in which the three phase of α, α' and γ coexist. The equilibrium condition of annealed

(13) The heterogeneous field in the Fe-Ni system is due to the result which was dilatometrically determined by Dr. K. Honda. (Sci. Rep. Tôhoku Imp. Univ. **16** (1927) 745.)

(14) Recently an X-ray investigation of the ternary system Fe-Ni-Al at room temperature has been reported by A. J. Bradley and A. Taylor. Their result agrees with the present author's work. (Cf. Nature, **140** (1937), 1012; also Proc. Roy. Soc. London, **166** (1938), 353.)

specimens at room temperature can not be obtained. The deviation from linearity of the boundary of the three phase region ($\alpha+\alpha'+\gamma$) above mentioned is probably attributed to this difficulty. (In the diagram formerly proposed the abrupt change of curve was overlooked, and consequently the heterogeneous portion of this system consisted simply of α- and γ-phase).

The phase boundaries of the heterogeneous field as well as the trigonal domain of the ($\alpha+\alpha'+\gamma$)-phase at various temperatures were then examined by quenching. Points showing the abrupt change of curves, which mark the heterogeneous field, are the corners of the three phase region, and are only observable below 1200°. In the space model of ternary diagram they form as their loci a space curve, which indicates a eutectoid reaction in this ternary system; α-solid solution and α'-solid solution begin to separate out from each other below 1200°, till the eutectoid reaction occurs, at which temperature the separation of γ-phase begins to take place.

From the experiments above described the constitution of the iron-rich iron-nickel-aluminium system has been constructed. In the space model of this diagram an ovaloid due to the ($\alpha+\alpha'$) field comes out. This ovaloid denotes the precipitation of a body-centered cubic solid solution (α') from the homogeneous solid solution, while the surface which bound the heterogeneous field of ($\alpha+\gamma$) indicates the precipitation of a face-centered cubic solid solution (γ) from the homogeneous solid solution. These two surfaces intersect in a space curve which is the line of a eutectoid reaction in this ternary system. This line is a part of the loci of vertices of the triangles representing the region of the ($\alpha+\alpha'+\gamma$)- field at temperatures below 1200°.

The particular account of this diagram will be given later.

§ 9. Some notes on the X-ray investigation.

The results of X-ray investigation of R. Glocker, H. Pfister and P. Wiest[3] as well as that of W. G. Burgers and J. L. Snoek[4] rest on

the diagram proposed by W. Köster[1]. They studied the crystal structure of the iron-nickel-aluminium magnet alloys and concluded that these alloys separate out γ-phase (a face-centered cubic lattice) from the matrix of α-phase (a body-centered cubic lattice). They also studied the width of the X-ray interference lines and explained the observed phenomena as the result of preliminary stage of the γ-precipitation.

The differentiation of α- and α'-phases is very difficult and in the author's early experiment[5] the iron-nickel-aluminium magnet alloys showed only the α-phase, the $\alpha \rightarrow \alpha+\alpha'$ change being unobserved. By ordinary annealing process of lump specimens the equilibrium condition can be attained with great difficulty, and hence in X-ray analysis to differentiate the α'-phase from the α-phase is very difficult. As the α-phase is of a body-centered cubic lattice and the α'-phase is also of a body-centered cubic lattice with a slightly larger lattice constant, the $\alpha \rightarrow \alpha+\alpha'$ change will result the split of the X-ray interference lines into two lines. But when the $\alpha \rightarrow \alpha+\alpha'$ change are incomplete, the split of the interference lines will be also incomplete. Thus by the ordinary heat treatment the split interference lines can not be easily recognised.

According to the author's early experiment it so happend that specimens which were investigated were those which lie in the $(\alpha+\alpha'+\gamma)$-field in Fig. 12, and those which belong to the $(\alpha+\alpha')$-field were not used at all. Thus the author observed the precipitation of only γ-phase in the iron-nickel-aluminium alloy. But the amount of the γ-phase which was precipitated was too small, by taking all the precipitated phase as the γ-phase, and by further experiment it turned out that some specimens, in which the precipitated phase was supposed to reveal the X-ray interference lines (both by the quantity and grain size), showed no evidence of γ-precipitation. Thus it became doubtful to suppose that the precipitated phase was simply γ-phase[5].

The width of the interference lines, which occurs when the alloys are tempered, was supposed by the former reporters[3][4] as the

result of the intermediate state of γ-precipitation, but there are some difficulties in this explanation. According to the author's investigation, the width of the interference lines increases monotonously when the tempering process is increased; while the hardness and the values of coercive force increase at first and then decrease. If the width of the interference lines is entirely due to the preliminary state for the γ-precipitation, then it ought to have a maximum width in the course of tempering. As will be easily seen from § 4 the width of the interference lines is partly due to the heterogeneous concentration which is caused by the $\alpha \rightarrow \alpha + \alpha'$ change, and hence when the tempering process is increased, the width of the interference lines will increase monotonously. (The increase of hardness and the values of coercive force is due to the preliminary state of the precipitation phenomenon, and hence hardness and coercive force show a maximum value in the tempering process.) The width of the X-ray interference lines can be easily explained by the diagram proposed by the present author. By powder-annealing in vacuum the diffusion in the quenched iron-nickel-aluminium alloys was accelerated, and as the result of the $\alpha \rightarrow \alpha + \alpha'$ change in the alloys the interference lines belonging to a body-centered cubic lattice splitted into two as shown in Figs. *7 a*, *7 b*, *7 d*, and *7 e*. Of these two body-centered cubic lattices that of the smaller lattice constant (α-phase) is the solid solution of α-iron, and that of the larger lattice constant (α'-phase) showing the superlattice lines of (001), (111) etc. is considered to be the solid solution of NiAl. The particular account of X-ray analysis will be later given.

§ 10. Change of the magnetic properties by heat treatment.

The effect of magnetic properties of a specimen (Fe 60%, Ni 28%, Al 12%) on heating is shown in Fig. 13. This alloy has a coercive force of 450 gauss in cast state, and it increased about 10 per cent by

subsequent annealing at 650° for an hour. By quenching the same specimen from 1300° in water, the coercive force decreases and by subsequent tempering it increases remarkably. This change is illustrated in Fig. 13.

It is to be noted that the annealing temperature at which the specimens show the maximum values of coercive force depends very much on the previous heat treatment. The maximum value of coercive force of quenched specimen was shown by the specimen tempered at 700°, while that of the cast by the specimen annealed at 650°, the values of the coercive force being 310 Gauss and 490 Gauss respectively. In order to obtain the maximum values of coercive force, the quenched specimens were always heated about 50° higher than the cast specimens, the maximum values of the coercive force always being greater in the latter.

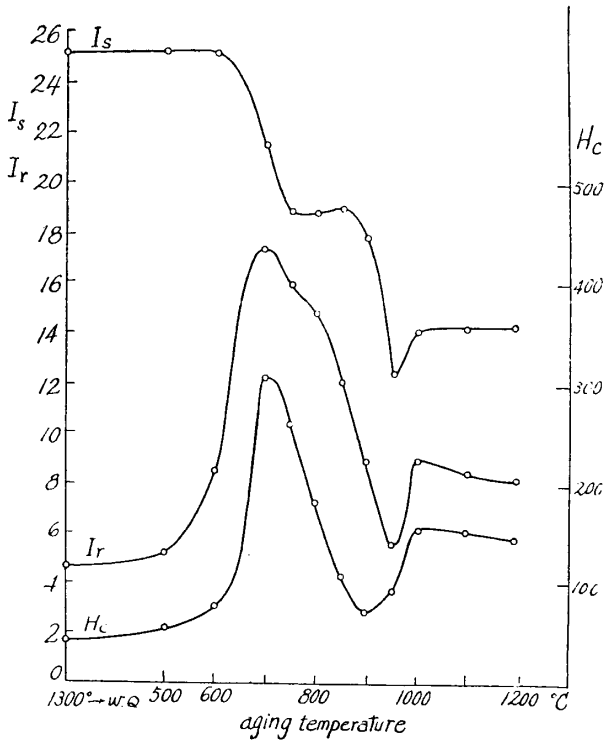

Fig. 13.

The maximum value of the coercive force of iron-nickel-aluminium magnet alloys, on the other hand, is influenced by the cooling velocity[15] of the specimen in the casting as is shown in Fig. 14, which shows the change observed by varying the temperature of the mould. Thus by heating the mould to 400°~500°, the specimens were prepared.

(15) W. S. Messkin, B. E. Somin: Eigenschaften von Nickel-Aluminium-Magnetstahl. Arch. Eisenhüttenwes., 8 (1935), 315.

§ 11. Investigation of the coercive force of the iron-nickel-aluminium alloys.

The results of the present work on the coercive force of the iron-nickel-aluminium alloys are shown in Fig. 15. It is seen that the composition of the iron-nickel-aluminium magnet alloys lies in the $(\alpha+\alpha')$- and $(\alpha+\alpha'+\gamma)$-fields in Fig. 12. Further it also lies in the homogeneous α-phase at higher temperatures. Hence it may be said that the iron-nickel-aluminium magnet alloys solidify from the melt as α-solid solution and with lowering of temperature it separates out the solid solution of NiAl, resulting in the coexistence of two body-centered cubic lattices $(\alpha+\alpha')$, and some of them further separate the γ-phase of nickel by a eutectoid reaction.

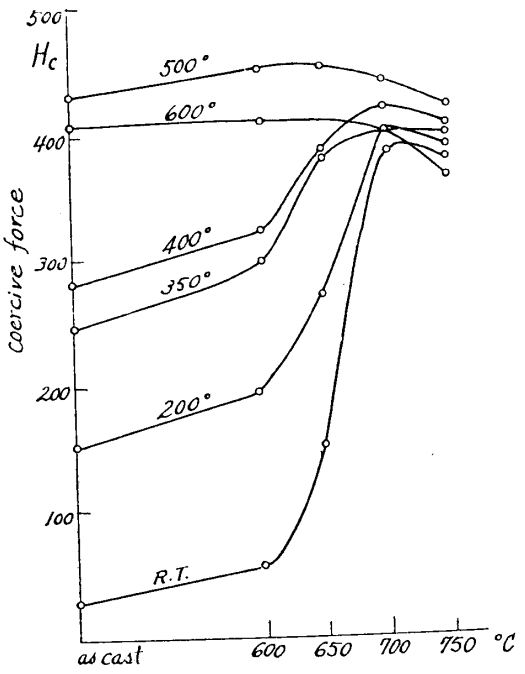

Fig. 14.

Next two specimens are considered, one belongs to the $(\alpha+\alpha')$-field while the other belongs to the $(\alpha+\alpha'+\gamma)$-field in Fig. 12. The former contains 53 percent iron, 35 per cent nickel and 12 per cent aluminium (Specimen A) and the latter contains 55 per cent iron, 35 per cent nickel and 10 per cent aluminium (Specimen B). In X-ray analysis specimen A showed only two body-centered cubic lattices and specimen B two body-centered cubic lattices and a small amount of a face-centered cubic lattice. Comparing the coercive force of these two specimens, it is seen from Fig. 15 that specimen A has larger coercive force than specimen B. Hence it may be said that the specimen having larger coercive force does not

show the separation of γ-phase at all. This relation holds good for alloys of any nickel content, and it may be well said that the composition of typical iron-nickel-aluminium-magnet alloy lies in the $(\alpha+\alpha')$-field in Fig. 12.

By microscopic and X-ray analyses it is seen that the precipitation phenomenon does not occur when the coercive force is increasing, and hence the structure of the iron-nickel-aluminium magnet alloy is in the intermediate state under immense strain prior to the precipitation of α'-phase from the matrix of α-phase.

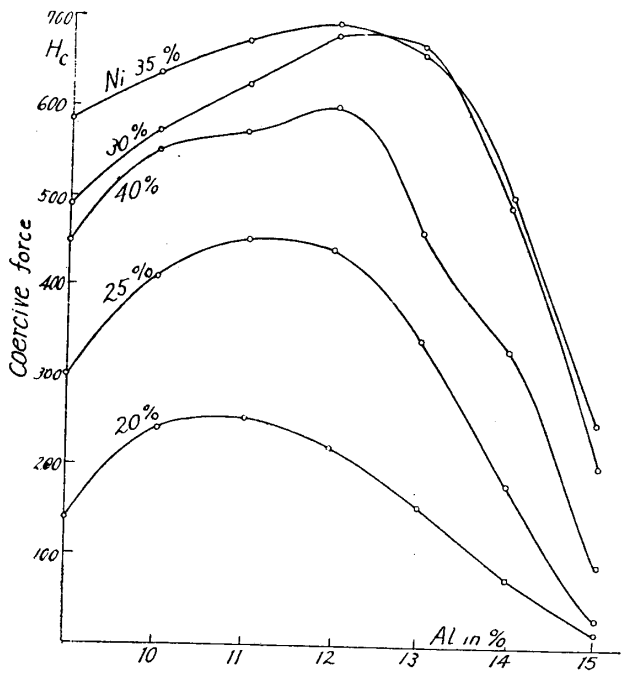

Fig. 15.

§ 12. Conclusions.

By X-ray and microscopic analyses the constitutional diagram of the iron-rich iron-nickel-aluminium system was constructed, and a new phase α', which was identified as the solid solution of NiAl, was introduced. The heterogeneous field in this system consists of four parts; $(\alpha+\gamma)$, $(\alpha+\alpha')$, $(\alpha'+\gamma)$ and $(\alpha+\alpha'+\gamma)$. The coexistence of two body-centered cubic lattices due to the $\alpha \rightarrow \alpha+\alpha'$ change as well as the occurrence of the heterogeneous field $(\alpha+\alpha'+\gamma)$ were confirmed by X-ray analysis. Further, by the measurement of the coercive force of the iron-nickel-aluminium alloys, the conclusion is drawn that the large coercive force shown by these alloys is mainly due to the $\alpha \rightarrow \alpha+\alpha'$ change.

In conclusion the author wishes to express his hearty thanks to Dr. K. Honda, President of the Tôhoku Imperial University, for his kind guidance. Sincere thanks are also due to Dr. T. Kobayasi, Professor of the Aeronautical Research Institute, Tôkyô Imperial University, for his kind guidance and constant encouragement during the course of the present investigation.
